

Experimental study of forced and freely decaying wall bounded MHD turbulence, at low R_m

BAKER^{1,2} Nathaniel, POTHÉRAT² Alban, DAVOUST³ Laurent, DEBRAY⁴ François.

Affiliation: ¹ CNRS CRETA – 38042 Grenoble – France

² AMRC, Faculty of Eng. and Comp., Coventry University – Coventry CV1 5FB - UK

³ SIMAP, EPM Group – 38402 Saint Martin d'Hères – France

⁴ LNCMI, CNRS-UPS-INSA-UJF – 38042 Grenoble – France

e-mail address of corresponding author: nathaniel.baker@creta.cnrs.fr

Abstract: We investigate experimentally the properties of low- R_m MHD turbulence, which takes place in a wall bounded domain. First, we look at forced turbulence and show that it is possible to observe turbulent velocity fluctuations featuring 2D behaviour (in the sense that they do not depend on a spatial coordinate), even though a strongly 3D mean flow exists. Second, we analyse the free decay of the turbulence, during which we can distinguish several distinctive regimes.

Introduction

One of the main features of MHD flows is the action of the Lorentz force, which tends to damp momentum along the magnetic field. This process can be interpreted as a diffusion of momentum along the magnetic field [1], eventually bringing the flow towards a two-dimensional state. Until now, most studies - whether experimental ([2], [3]), theoretical [4], or numerical [5] - have focused on cases where turbulence evolves in a space featuring either a free surface, infinitely distant boundaries, or periodic boundary conditions. However, the presence of obstacles is an intrinsic feature of real flows, and any attempt to fully explain their dynamics must account for them. The purpose of this study is to understand the effects of walls on the dynamics of electrically-driven low- R_m MHD turbulence. This paper breaks down into three parts: we will start by presenting our experimental setup, before analyzing the statistical properties of the fully developed turbulent flow, and finally looking at the dynamics of its free decay.

1. Experimental methods

Our work was conducted using the Flowcube, an experimental rig designed to generate and investigate electrically driven turbulence in a closed cubic domain [6]. It consists of a frame of inner length $L = 100$ mm closed by electrically insulating side plates. Instruments are embedded flush within each one of these plates in order to either drive the flow (current injection electrodes) or analyze its properties (potential probes and ultrasound transducers). The cube is placed inside the 450 mm bore of a superconducting magnet, which applies a vertical magnetic field $B_0 \mathbf{e}_z$ of up to 4T. The cube is filled with Gallinstan, an eutectic alloy of gallium, indium and tin, which is liquid at room temperature, and characterized by a density $\rho = 6400$ kg/m³, a kinematic viscosity $\nu = 4 \times 10^{-7}$ m²/s and an electrical conductivity $\sigma = 3.4 \times 10^6$ S/m. Electrical current is injected by means of a 10×10 square array of electrodes, alternately connected to the positive and negative poles of a DC power supply. The injection electrodes are located on the bottom plate, and are uniformly separated by a distance $l^i = 10$ mm from each other. 100 uniformly spaced potential probes mesh a 30 mm x 30 mm square area located on the bottom plate with a spatial resolution $\Delta x = 2.5$ mm. These probes give access to the electric potential field at the plate's surface, from which can be deduced the velocity field perpendicular to the magnetic field in the plane right above the bottom Hartmann layer [7]. Finally, a vertical row of ultrasound transducers give horizontal velocity profiles at different heights along the magnetic field. The spatial domain explored by the transducers spans from $x = 10$ mm to $x = 90$ mm (the immediate vicinity of the side walls must be ignored as the signals are corrupted by strong echoes), with a spatial resolution $\Delta x = 0.22$ mm.

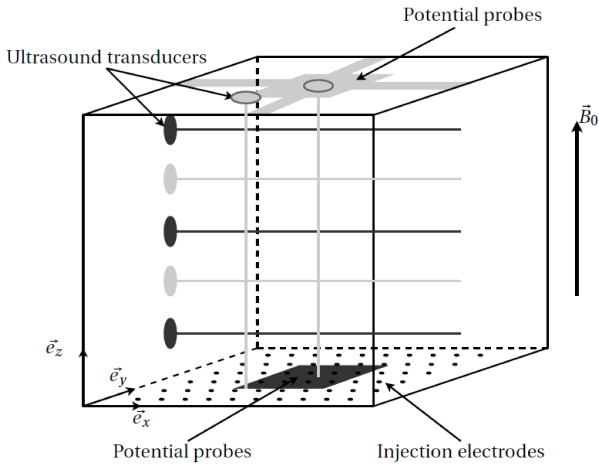


Figure 1: Sketch of the Flowcube. Electrical current is injected through the injection electrodes at the bottom. The data acquired in sections 2 and 3 come from the probes colored in dark gray (left ultrasound transducers and bottom potential probes respectively). Probes colored in light gray are present in the experiment but not exploited in this paper.

The operating conditions used for the experiments are characterized by a Hartmann number $Ha \sim 7300$ and a Reynolds number based on the turbulent fluctuations $Re \sim 30000$. A total electrical

current $I = 300$ Amps was injected. These parameters were selected for two reasons: first, they yield a strongly three-dimensional forced flow, where inertia and the Lorentz force are in strong competition. Second, they lead to a reasonably long decay (around 15 seconds), which is easy to capture. The forcing was even and carefully monitored during the measurements. During a typical experimental run, the forced state was recorded for 3 minutes after the transient regime vanished (almost instantly). The decay was then triggered by suddenly switching off the power supply. The recording was kept running during 30 seconds after the decay had been triggered.

2. Forced Turbulence

In this section, we analyze the statistical properties of forced turbulence. The data presented below result from averaging 35000 velocity profiles (50 experimental runs, during which 700 forced profiles were recorded).

Figure 2 shows the normalized mean flow and turbulent fluctuations horizontal profiles, at different locations away from the forcing. Figure 2.a's bottom signal features a quasi periodic profile, whose half wavelength is $l^i = 10$ mm. This length corresponds to the spacing between injection electrodes and can be interpreted as the characteristic length of the forcing. The peaks and troughs are therefore evidence of counter rotating structures generated by the forcing. As we move up in the box, one can see that the amplitude of the mean flow, relative to the bottom flow decreases dramatically with height. In fact, there appears to be a factor 10 between the bottom flow where the forcing takes place and the top flow. This behavior can be put on account of the Lorentz force not being strong enough to compete with inertia throughout the box, therefore leading to strong three-dimensionality [8]. Figure 2.b, shows that the intensity of the fluctuations at the bottom features strong spatial variations. Those variations are quickly damped along z , giving a rather even and uniform fluctuation distribution far from the forcing area. Contrary to the mean flow, the amplitude of the fluctuations is not damped with height, and seems to be affected by side walls only.

Figure 3 gives a synthesized view of the previous argument. In particular, figure 3.a shows how quickly the mean flow is damped along z , resulting in a very weak residual flow for $z > 50$ mm. In the same spirit, 3.b shows how the intensity of fluctuations is smoothed out and become constant for $z > 50$ mm. In other words, horizontal turbulent fluctuations seem to feature a 2D behavior (in the sense that they do not depend on the spatial coordinate z), although the mean flow is strongly three-dimensional. It is also worth noting that the fluctuations are much more intense than the mean flow at any given height. Indeed, they happen to be twice as important at the bottom, but become more than twenty times larger at the top.

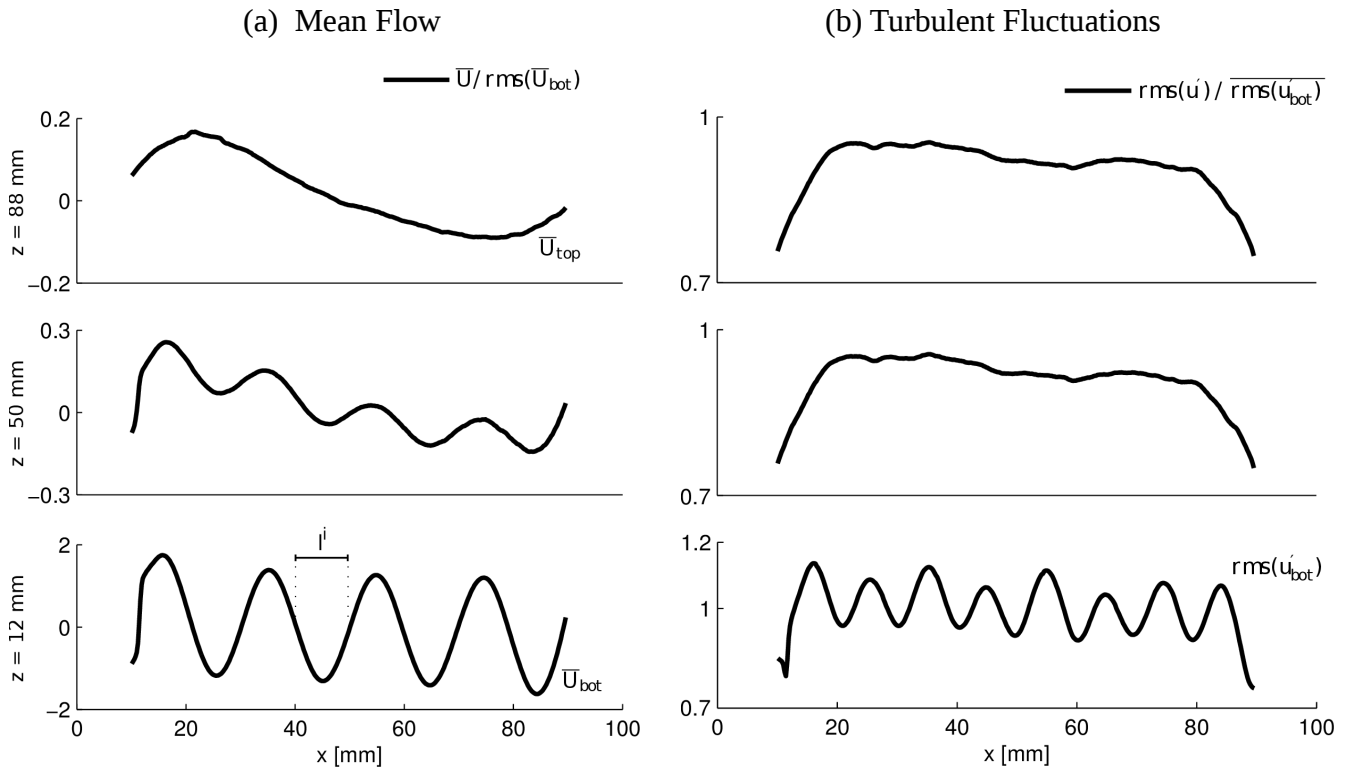


Figure 2: horizontal mean flow (left) and turbulent fluctuations (right) perpendicular to the magnetic field. Both graphs are normalized by the rms (resp. mean) of the bottom signal. Notice the damping of smaller structures by the Lorentz force along z .

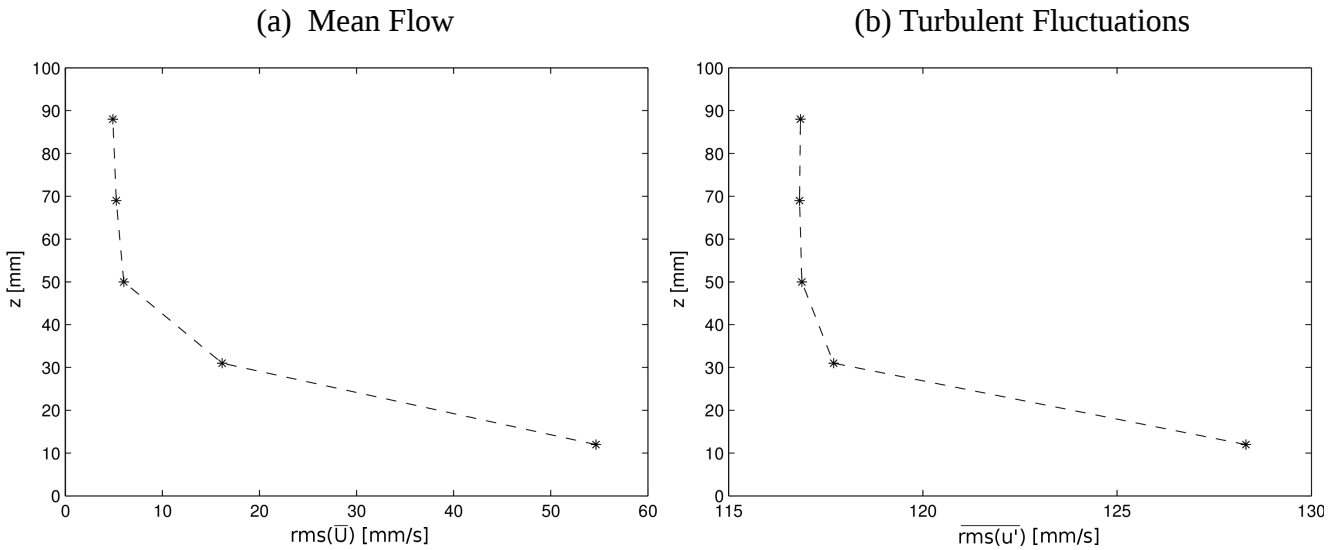


Figure 3: Statistical properties against height. Mean flow (left), turbulent fluctuations (right).

Figure 4 gives an alternate representation in Fourier space of the signals displayed earlier. The spectral examination of the velocity signals indicates how energy is distributed amongst the different scales along x . The bottom spectrum shows a peak (marked by the dotted line) corresponding to the scale $l^p = 19$ mm, which happens to be twice the spacing between electrodes, or in other words the size of a pair of counter rotating vortices. The energy therefore seems to be concentrated in this elementary pattern: the pair of counter-rotating vortices act as the energy injection scale in the experiment. Furthermore, the peak visible at the bottom (i.e. close to where the forcing takes place) does not appear elsewhere, meaning that the energy has been redistributed

amongst scales with height. It is also worth noting the various breaks in slopes that occur in these spectra, even though the underlying physical mechanisms remain to be determined. Nonetheless, the steep slopes at the right end of the spectra indicate that smaller scales receive very little energy.

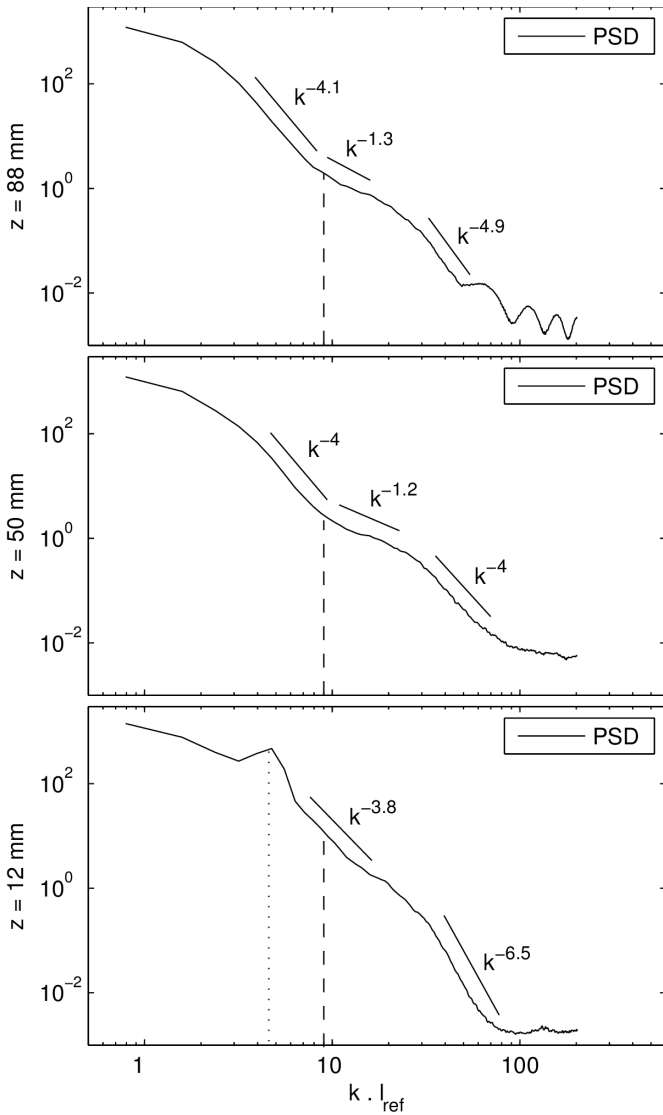


Figure 4: Power spectral density at three different heights. The x-axis is normalized by the length explored by the ultrasound transducers. In this case, $l_{ref} = 90$ mm. The spacing between injection electrodes is marked by the dashed lines, the energy containing scale is marked by the dotted line.

3. Decaying turbulence

Next, we turn our attention to freely decaying turbulence. The results shown in this section come from averaging over 50 different decays.

Figure 5.a displays the decay of the kinetic energy per unit volume contained in the bottom square $E(t)$, which is defined by :

$$E(t) = \sum_i \frac{u_i(t)^2}{2} .$$

In the previous formula, $u_i(t)$ refers to the i^{th} velocity value deduced from the bottom electric potential measurements at the given time t . The signal is normalized by $E(0)$, which refers to the same quantity, but evaluated during the forced state (i.e. right before the decay was triggered). Time is normalized by the Joule time $\tau_J = \rho / \sigma B_0^2$.

Figure 5.b shows the time decay of particular Fourier coefficients contained within the investigation area. In other words, we look at the decay of the energy for a given set of structures. Note however that since we are restricted to a 30 mm x 30 mm square sampled at 2.5 mm, we actually have access to a very limited range of scales contained within $5 \text{ mm} < l < 15 \text{ mm}$. These scales happen to be very close to the injection scale, which limits the extent of our study. Nonetheless, one can clearly identify three distinct regimes on both graphs: region (a) for $0 < t/\tau_J < 1500$, region (b) for $1500 < t/\tau_J < 5000$ and region (c) for $t/\tau_J > 5000$. As the decay goes on, the slopes of figure 5.a become steeper, meaning that energy gets damped more quickly. Looking at figure 5.b, region (a) is a region where energy dissipation very clearly depends on the scale. More specifically, the bigger structures seem to lose their energy faster than the smaller ones. In region (b), one can observe a very distinctive regime change, where the decay rate becomes scale independent. This regime exhibits a steady $t^{-1.5}$ decay law in agreement with figure 5.a. Region (c) can be referred to as the final stage of the decay. In this region the decay appears to become scale specific again, however unlike in the early decay, the structures whose energy is dissipated faster are now the smaller ones.

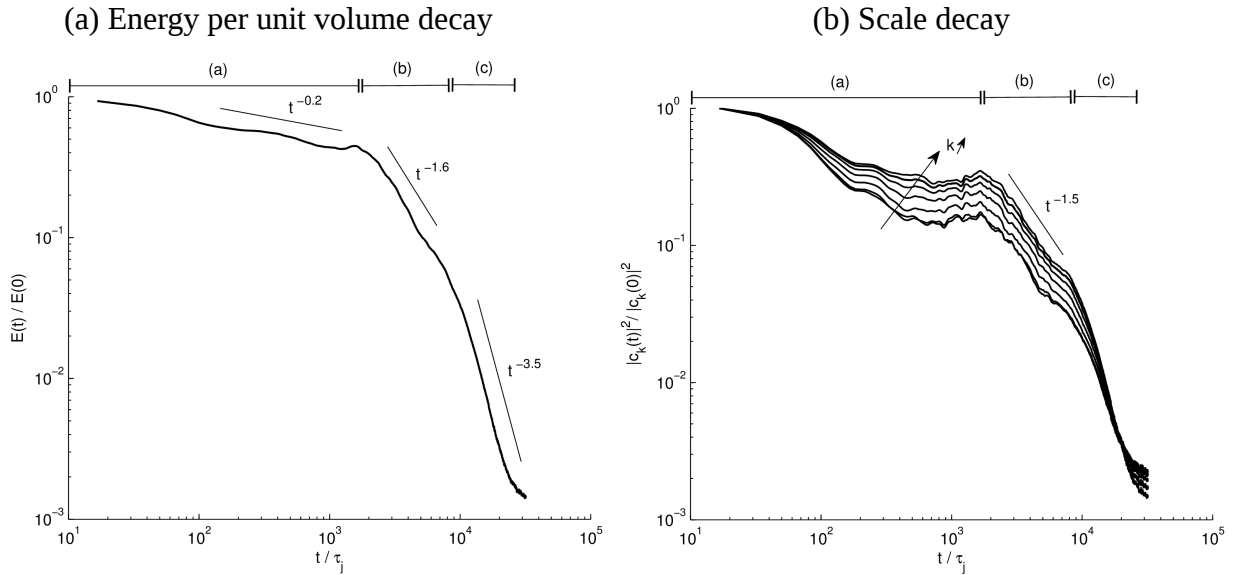


Figure 5: Decay of the kinetic energy per unit volume inside the middle square of the bottom plate. The time axis is normalized by the Joule time $\tau_J = 0.47$ ms, which is the shortest phenomenon occurring in the experiment. Time decay of Fourier coefficients, normalized by their respective value before the decay is triggered. The scales considered here are contained within the 30 mm \times 30 mm central square. The time axis is normalized by the Joule time. $k \sim 1/l$ is the wave number associated to the structure of size l .

4. Conclusion

We have presented different aspects of wall-bounded low-Rm MHD turbulence under $Ha \sim 7300$ and $Re \sim 30000$. In these conditions, we observed a forced mean flow presenting very strong three-dimensionality, characterized by a weak residual flow featuring large structures at the top of the box, despite strong forcing took place at small scales at the bottom. This behavior can be explained by the Lorentz force diffusing vorticity along the magnetic field, damping velocity gradients - thus smaller structures - along the magnetic field. This phenomenon translates into spectral space by various slopes whose physical meaning is still to be tackled. In addition, we obtained unprecedented results regarding the decay of wall-bounded MHD turbulence. Even though they are still very qualitative, we were able to clearly identify different phases where radically different physical phenomena are likely to occur.

The work presented here is still very much in progress, and many issues need to be addressed before we can give a definitive answer to what is happening during the decay. First, more decays must be measured until the results have fully converged. Second, it is necessary to analyze a broader range of structures, as those we were limited to are too close to each other. Last, we need to explore other operating settings, especially higher magnetic fields.

5. References

- [1] J. Sommeria and R. Moreau. *Journal of Fluid Mechanics*, 118:507–518, 1982.
- [2] J. Sommeria. *Journal of Fluid Mechanics*, 189:553–569, 1988.
- [3] B. Sreenivasan and T. Albuossière. *Journal of Fluid Mechanics*, 464:287–309, 2002.
- [4] H. K. Moffatt. *Journal of Fluid Mechanics*, 28(03):571–592, 1967.
- [5] O. Zikanov and A. Theiss. *Journal of Fluid Mechanics*, 358:299–333, 1998.
- [6] R. Klein and A. Pothérat. *Physical review letters*, 104(3), 2010.
- [7] A. Kljugin and A. Theiss. *Experiments in Fluids*, 25(4):298–304, 1998.
- [8] A. Pothérat and R. Klein. <http://arxiv.org/pdf/1305.7105v1.pdf>.